Time-resolved energy transfer from single chloride-terminated nanocrystals to graphene

O. A. Ajayi,[1,2,a)] N. C. Anderson,[3] M. Cotlet,[4] N. Petrone,[2] T. Gu,[1] A. Wolcott,[3] F. Gesuele,[1] J. Hone,[2] J. S. Owen,[3] and C. W. Wong[1,2,a)]

[1]Optical Nanostructures Laboratory, Center for Integrated Science and Engineering, Solid-State Science and Engineering, Columbia University, New York, New York 10027, USA
[2]Department of Mechanical Engineering, Columbia University, New York, New York 10027, USA
[3]Department of Chemistry, Columbia University, New York, New York 10027, USA
[4]Brookhaven National Laboratory, Upton, New York, New York 11973, USA

We examine the time-resolved resonance energy transfer of excitons from single n-butyl amine-bound, chloride-terminated nanocrystals to two-dimensional graphene through time-correlated single photon counting. The radiative biexponential lifetime kinetics and blinking statistics of the individual surface-modified nanocrystal elucidate the non-radiative decay channels. Blinking modification as well as a $4\times$ reduction in spontaneous emission were observed with the short chloride and n-butylamine ligands, probing the energy transfer pathways for the development of graphene-nanocrystal nanophotonic devices. © 2014 AIP Publishing LLC.
[http://dx.doi.org/10.1063/1.4874298]

Recent advances in ligand exchange techniques have paved the way for improved surface passivation of quantum dots.[1–3] In these techniques, long insulating organic ligands are replaced by short inorganic ligands. Recently, anionic halide ligands have been used to replace carboxylate ligands that balance the charge of the metal-rich nanoparticle surfaces, thus achieving charge-neutral nonstoichiometric particles without long chain organic surfactants.[4] These short compact halide ligands have been shown to effectively passivate midgap trap states in quantum dot films thus improving the open circuit voltage, leading to record power conversion efficiencies (8%).[5] Additionally, these short halide ligands are favorable for studies of the rich field of distant-dependent near field interactions.

Of particular interest are interactions between halide terminated quantum dots and two-dimensional materials,[6] which experience strongly enhanced coupling due to planar confinement and follow a d^{-4} distance scaling[7–9] at short distances where electron-hole pair interactions dominate. Since the isolation of single layer graphene,[10] there has been an explosion of research of purely two-dimensional materials due to the unique physics anticipated at this atomic scale.[11–17] Graphene, with its broadband transparency[18] and high carrier mobility,[19] provides a robust platform to explore light-matter interactions with photoexcited halide-terminated quantum dots. Additionally, graphene's mechanical flexibility encourages its application in the emerging class of flexible electronics. In the presence of graphene, a donor-acceptor interaction occurs providing competing pathways for photoluminescence through Förster-like resonant energy and/or charge transfer. Spectral overlap, electronic coupling, and proximity determine the kinetics of energy and charge transfer between the excited quantum dot and graphene. Resonant energy transfer occurs via dipole coupling to the two-dimensional plane of graphene with a z^{-4} distance

rate dependence.[6,19–21] Electronic excitation energy is transferred from the photoexcited dipole via Coulomb coupling to the graphene acceptor. Charge transfer is possible when suitable alignment occurs between the energy levels of the donor quantum dot and graphene acceptor.

Here, we study the near-field interactions between quantum dots passivated by non-insulating, inorganic ligands and graphene, which allows us to probe relaxation pathways relevant to nanophotonic devices such as photodetectors. We measure the radiative lifetime and blinking statistics of single chloride-terminated CdSe nanocrystals on large-area chemical-vapor-deposited (CVD) graphene to quantify the energy transfer rate and efficiency. A $4\times$ reduction in the radiative lifetimes of the photoexcited single halide-terminated nanocrystals was observed on graphene clad glass substrates versus bare glass, corresponding to an energy transfer rate of $2.37 \times 10^8\,\mathrm{s}^{-1}$.

Chloride-terminated nanocrystals were synthesized by cleaving the native long carboxylate ligands on core-only 3.3 nm CdSe nanocrystals as detailed in Ref. 4. The resulting nanocrystals (Scheme 1) are passivated with chlorine ligands which balance the charge of the metal rich core and n-butylamine ligands (0.6 nm in length), which maintain the solubility of the nanocrystals. Absorption and PL spectra of the chloride-terminated nanocrystals are provided in Figure 1(a). The short distance ($\sim$2.3 nm) from the n-butylamine bound nanocrystal center to graphene facilitates greater dipole energy transfer compared to $\sim$4.5 nm from conventional oleic-acid capped nanocrystals of the same core diameter.

We probe the near field interactions between chloride-terminated nanocrystals and graphene by measuring the temporally resolved fluorescence of the nanocrystals on graphene-clad glass substrates and bare glass substrates. The comparative quenching of the fluorescence on graphene provides a measure of the non-radiative decay rate as will be discussed. Figure 1(b) shows the Raman spectra of the CVD graphene at different positions, confirming uniformity of

a)Electronic addresses: oaa2114@columbia.edu and cww2104@columbia.edu
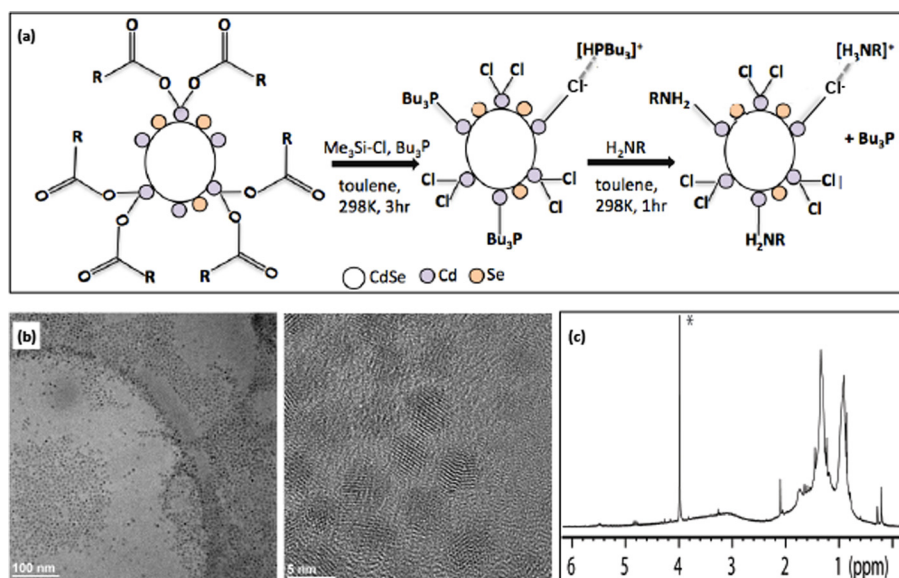
SCHEME 1. Chemical synthesis and characterization of chloride-terminated CdSe nanocrystals. (a) Schematic depiction of nanocrystal synthesis.[4] (b) High-resolution transmission electron micrographs of CdSe-CdCl$_2$/RNH$_2$ nanocrystals. Left scale bar: 50 nm. Right scale bar: 5 nm. (c) ^{1}H nuclear magnetic resonance spectrum of CdSe-CdCl$_2$/RNH$_2$ with ferrocene standard.

monolayer graphene. Figure 2 compares the photoluminescence of individual chloride-terminated nanocrystals on graphene-clad glass and bare glass substrates, both pumped at 2 μW averaged power with 90 ps pulses at 440 nm. On bare glass, single nanocrystals were more easily discernible with ~170 counts per millisecond, while on graphene, the photon counts from the single nanocrystals are lower, ~100 counts per millisecond. Photon collection at the individual or few nanocrystal level allows us to gain insight into the exciton radiative and non-radiative relaxation rates[22,23] which can be masked by ensemble inhomogeneous broadening. As shown by the circled points of interest in Figure 2, individual nanocrystals were selected for lifetime measurements.

Individual nanocrystals are known to exhibit "blinking" behavior[24–26] with distinct "on" and "off" photoluminescence intensity states that can be characterized by probability distributions of their *on*-times [$P(t_{on})$] and *off*-times [$P(t_{off})$]. The probability distributions are modeled as power laws,[27] with the off-times described by $P(t_{off}) = At_{off}^{-m_{off}}$ and the on-times

described by a truncated power law, $P(t_{on}) = At_{on}^{-m_{on}} e^{-t_{on}/\tau_{on}}$. Figure 3 shows representative photoluminescence intensity traces of the individual chloride-terminated nanocrystals on comparative graphene and glass substrates, with a $\Delta t = 10$ ms binning window.

We confirm the presence of individual nanocrystals using power law statistics. The characteristic exponents for the off- and on-time distributions are extracted using a log-log least squares fitting method. For the off-time distribution, m_{off} is found from the linear least-squares fitting of log[$P(t_{off})$] versus log[t_{off}] and for the on-time distribution, t_{on} (saturation time) and m_{on} are found from the least squares fitting to log[$P(t_{on})$] versus log[t_{on}]. Our results in Figures 3(b) and 3(c) show that the character of these individual chloride surface-modified nanocrystals (on glass) are in rough agreement with the τ_{on}/τ_{off} exponents of conventional spherical nanocrystals at this binning time.[28] We also observe a smaller τ_{on}, which is expected because τ_{on} decreases with the square of the applied power:[29] here we utilize a stronger pump power (2 μW) due to the low quantum yield (~3%) of these modified quantum dots at nanomolar concentration of amine. The chloride-terminated nanocrystals on CVD graphene demonstrated different blinking statistics as compared to glass as shown in Figures 3(f) and 3(g). Characteristic blinking is not observed on CVD graphene as is evident from the *poor* log-
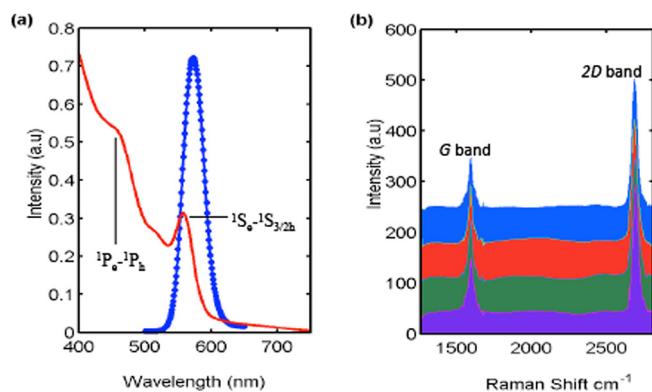

FIG. 1. Spectroscopic characterization of the chloride-terminated nanocrystals and graphene. (a) Photoluminescence emission for the chloride-terminated nanocrystals, with peak intensity at 573 nm and first excitonic transition at 558 nm. (b) Raman spectra of CVD graphene on glass, for four different spatial positions superimposed. The *G* and *2D* optical phonon bands homogeneity (centered at 1593 $\pm$ 2.2 nm and 2689 $\pm$ 3.9 nm, respectively), single *G* peak linewidth symmetry, and linewidths (*G* band full-width half-maximum of 30.75 $\pm$ 4.9 nm and *2D* band full-width half-maximum of 44.65 $\pm$ 2.5 nm) indicate single layer graphene with good uniformity.
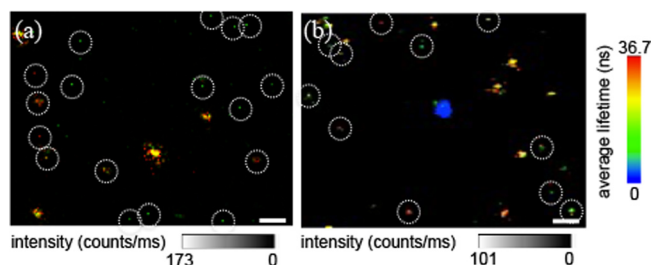

FIG. 2. Single chloride-terminated nonstoichiometric nanocrystal photoluminescence spectroscopy: (a) single chloride-terminated nanocrystal on glass, pump excitation 2 μW, (b) single chloride-terminated nanocrystal on graphene, pump excitation 2 μW. The single nanocrystal photon counts are higher on glass (~170 counts per millisecond) versus on graphene (~100 counts per millisecond). Scale bar: 500 nm.
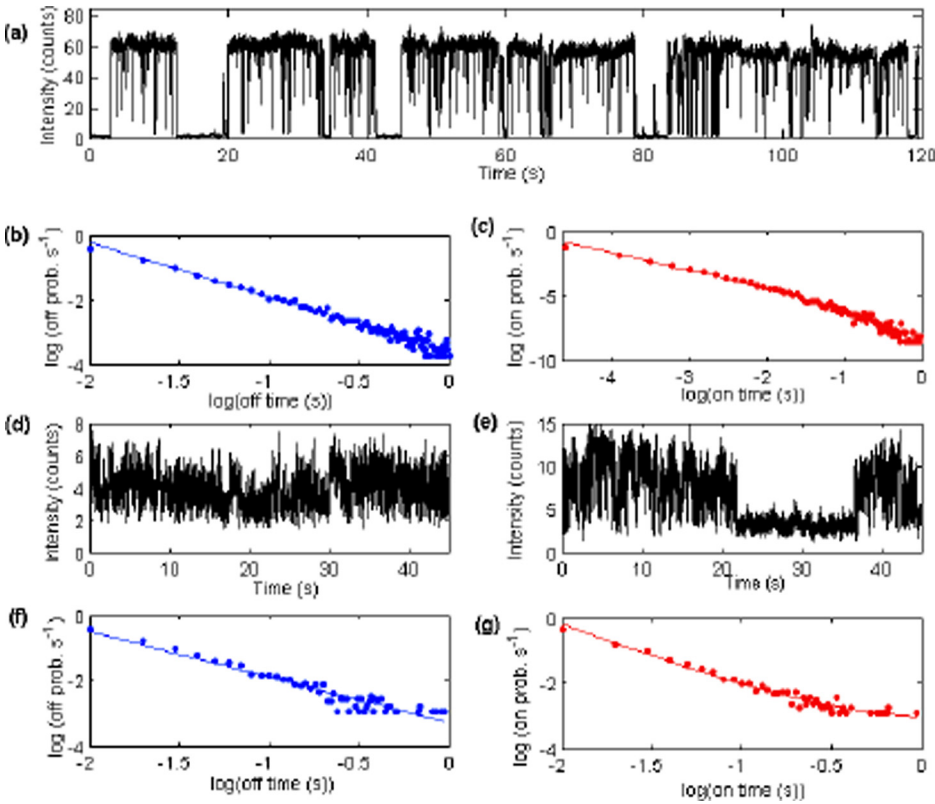
FIG. 3. Blinking statistics of single chloride-terminated quantum dot on glass and graphene, (a) representative intensity time trace of nanocrystal on glass. (b) Off-time probability distribution (1/s) on glass $P(t_{off}) = At_{off}^{-m_{off}}$, $m_{off} = 1.7$. (c) On-time probability distribution on glass $P(t_{on}) = At_{on}^{-m_{on}} e^{-t_{on}/\tau_{on}}$, $\tau_{on} = 1.28$, $m_{on} = 0.5$. (d) and (e) intensity time traces of nanocrystal on graphene. (f) Off-time probability distribution on graphene $P(t_{off}) = At_{off}^{-m_{off}}$, $m_{off} = 1.4$. (g) On-time probability distribution on graphene $P(t_{on}) = At_{on}^{-m_{on}} e^{-t_{on}/\tau_{on}}$, $\tau_{on} = 0.48$ and $m_{on} = 2.3$.

log fit to the expected power law distribution for the on $(P(t_{on}) = At_{on}^{-m_{on}} e^{-t_{on}/\tau_{on}})$ and off $(P(t_{off}) = At_{off}^{-m_{off}})$ times. Instead, varied fluctuations in intensity are observed in our measurements, as shown in Figures 3(d) and 3(e). The causes of the fluctuations are not completely understood, but we believe that the surface states of the chloride-terminated nanocrystals play a role in varied fluctuations.

To rigorously quantify the energy transfer and quenching (especially in the presence of blinking), we examined the radiative lifetime of the individual surface-modified nanocrystals on graphene. The energy transfer rate, k_{et}, and quenching can be experimentally determined from $k_{et} = \frac{1}{\tau'_{obs}} - \frac{1}{\tau_{obs}}$, where τ_{obs} is the radiative lifetime of the dipole on glass and τ'_{obs} is the radiative lifetime on graphene. The quenching (energy transfer rate) is of the form of Fermi's Golden Rule, where de-excitation of the photoexcited nanocrystal and subsequent electronic excitation of graphene is driven by Coulomb dipole interactions of the nanocrystal and graphene. Several theoretical models have been developed to account for the near-field interaction of graphene and an excited emitter, confirming a $1/z^4$ distance dependence where z is the mean distance between the dipole center and the graphene surface. As with absorption,[30] the fine structure constant has been shown to be central to a universal scaling law of energy transfer in graphene,[7] yielding a simple and powerful relation. We adapt this scaling to yield a calculated energy transfer rate, k_{cal}, described by

$$k_{cal} \approx \frac{1}{\tau_o} \left[\frac{9v\alpha}{256\pi^3 (E+1)^2} \left(\frac{\lambda_0}{z} \right)^4 \right], \qquad (1)$$

where v is a dipole orientation constant, $v = 1$ and $v = 2$ for parallel and perpendicular dipole orientation, respectively,

λ_0 is the free-space emission wavelength of the emitter, E is the permittivity of the bulk medium (glass in this case), α is the fine structure constant, and τ_o is the radiative lifetime of the emitter in vacuum.

As shown in Figure 4, a biexponential lifetime decay was observed for individual chloride-terminated nanocrystals on both glass and graphene. The biexponential lifetime decay of these individual nanocrystals on glass can be attributed to fine splitting of the optical transitions in CdSe nanocrystal due to stochastic ground state dipole moments. These dipole moments arise from imperfect surface passivation.[31] With these chlorine-terminated quantum dots, imperfect surface passivation is in part due to the tendency of the amine ligands to dissociate from the nanocrystal surface at low ligand concentration in solution[32] and also to their slow evaporation from the nanocrystal surface when the nanocrystals are deposited on the substrate. The fast lifetime component (τ_1) of the lifetime decay is attributed to recombination of the populated core-state (surface states) while the slow lifetime component (τ_2) is attributed to exciton recombination.[33]

On graphene, both τ_1 and τ_2 components of the biexponential lifetime are shortened, as summarized in Figure 4(b). This enhanced lifetime quenching is indicative of energy transfer of the excitons into graphene that is competitive with the present relaxation pathways: surface trap and exciton recombination.[33] The reduction of nanocrystal blinking on graphene further confirms that the energy transfer rate exceeds that of the competing pathway of photo-induced electron trapping rate of the blinking state.[6,34] With an amplitude-weighted average of the τ_1 and τ_2 lifetime components (given by $\tau = \sum_{i=1}^{n} \frac{A_i \tau_i}{\sum A_i}$), we observed an average lifetime τ of 13.2 ns (σ: 7.2 ns) on glass and 3.2 ns (σ: 2.2 ns) on graphene. This is also illustrated in Figure 4 and is a
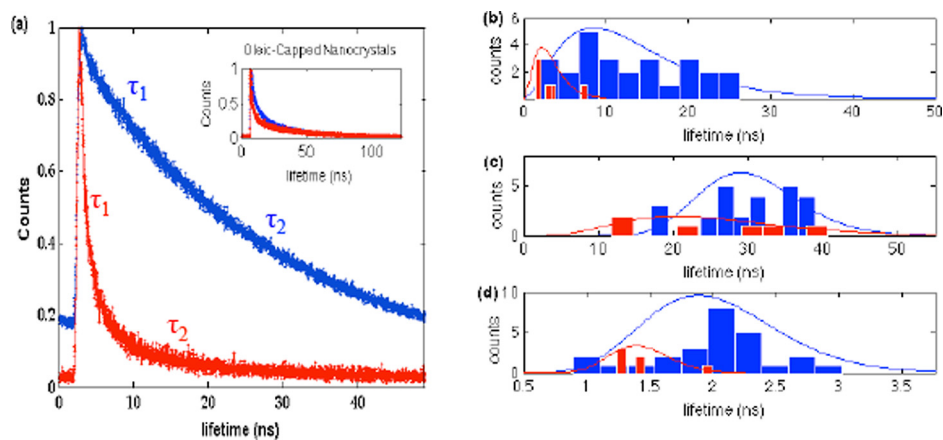
FIG. 4. Time-resolved lifetime measurements of single chloride-terminated nanocrystal on glass (blue) and graphene (red). (b)–(d) Distribution of lifetime components fit to Gamma distribution, (a) representative lifetime traces of single chlorine-terminated nanocrystal on glass and graphene. Inset: representative lifetime traces of single oleic-capped nanocrystals on glass and graphene, (b) distribution of weighted lifetime on glass and graphene (chlorine-terminated nanocrystals). (c) Distribution of long lifetime component (τ_2) on glass and graphene (chlorine-terminated nanocrystals). (d) Distribution of short lifetime component (τ_1) on glass and graphene (chlorine-terminated nanocrystals).

$4\times$ reduction in the spontaneous emission lifetime. We note that the average τ_1 on glass and graphene are 2.03 ns (σ: 0.50 ns) and 1.42 ns (σ: 0.28 ns), respectively. The average τ_2 on glass and graphene are 30.49 ns (σ: 6.37 ns) and 25.31 ns (σ: 11.46 ns), respectively. With the amplitude-weighted lifetime, we obtain an experimentally observed resonant energy transfer rate of $2.4 \times 10^8 \, s^{-1}$. This yields an energy transfer efficiency ($\eta = 1 - \tau/\tau_o$) of 76%.

For direct comparison, we also investigated the energy transfer between similarly sized CdSSe/ZnS nanocrystals (emission 578 nm) onto graphene as shown in the inset of Figure 4. We expect the longer length of the oleic acid ligands terminating the nanocrystals to reduce energy transfer. We observe a $2.5\times$ reduction in the spontaneous emission lifetime of these oleic acid capped nanocrystals (average lifetime on glass: 13.87 ns, σ: 10.79 ns and average lifetime on graphene: 5.46 ns, σ: 2.6 ns), corresponding to an energy transfer rate of $1.11 \times 10^8 \, s^{-1}$. A biexponential decay is also observed with the oleate-terminated nanocrystals. Here the average τ_1 on glass and graphene are 6.14 ns (σ: 5.75 ns) and 3.11 ns (σ: 0.92 ns), respectively. The average τ_2 on glass and graphene are 33.01 ns (σ: 6.13 ns) and 31.76 ns (σ: 8.77 ns), respectively.

We note that the calculated rate of energy transfer ($2.4 \times 10^8 \, s^{-1}$) from chloride-terminated nanocrystals onto graphene is on par with dipole-dipole transfer in nanocrystal assemblies[35] and nanocrystals on graphene-derived surfaces,[36,37] albeit lower than intensity-derived energy transfer measurements of well-passivated core-shell nanocrystals on graphene[6] and recent molecule-graphene studies.[7] The ideal theoretical resonant energy transfer rate (from Eq. (1)) is $4.0 \times 10^{10} \, s^{-1}$ for the parallel dipole orientation ($k_{//}$) and $8.1 \times 10^{10} \, s^{-1}$ for the perpendicular dipole orientation ($k_\perp$), yielding a dipole-averaged [$k = (2/3)k_{//} + (1/3)k_\perp$] Förster energy transfer rate ($1/\tau_o$) of $5.4 \times 10^{10} \, s^{-1}$. Considering the additional distance added from the presence of residual poly-methyl-methacrylate (PMMA: $\sim$1 nm thickness), on the graphene surface, the theoretical resonant energy is adjusted to $1.28 \times 10^{10} \, s^{-1}$. The energy transfer efficiency can be improved with thorough removal of any residual films such as the PMMA film on graphene, reduction of impurities at the substrate-graphene interface through a dry transfer technique,[38] removal of the remaining alklyamines groups on the modified nanocrystal surface, and further passivation of the chloride-surface modified nanocrystals.

Our results have demonstrated significant near-field coupling between isolated surface-treated nanocrystals and larger-area monolayer CVD graphene. This study shows that considerable energy transfer rates ($2.37 \times 10^8 \, s^{-1}$) and energy transfer efficiencies (76%) are possible with chloride-terminated CdSe nanocrystals. Halide ligands are attractive for energy transfer applications because of their short length, however a trade-off exists between efficient coulombic coupling and surface stability. The high theoretical energy transfer rate greatly motivates further studies to optimize the ligand length towards improved energy transfer performance. Following these studies, numerous research areas are ripe for exploration with this system including plasmonics[8] and photo-detection.[39]

[1]Z. Lin, H. Li, A. Franceschetti, and M. Lusk, ACS Nano **6**(5), 4029 (2012).

[2]J. S. Owen, J. Park, P. E. Trudeau, and A. P. Alivisatos, J. Am. Chem. Soc. **130**, 12279 (2008).

[3]J. Tang, K. W. Kemp, S. Hoogland, K. S. Jeong, H. Liu, L. Levina, L. Furukawa, X. Wang, R. Debnath, D. Cha, K. W. Chou, A. Fischer, A. Amassian, J. B. Asbury, and E. H. Sargent, Nature Mater. **10**, 765 (2011).

[4]N. C. Anderson and J. S. Owen, Chem. Mater. **25**, 69 (2013).

[5]A. H. Ip, S. M. Thon, S. Hoogland, O. Voznyy, D. Zhitomirsky, R. Debnath, L. Levina, L. R. Rollny, G. H. Carey, A. Fischer, K. W. Kemp, I. J. Kramer, Z. Ning, A. J. Labelle, K. W. Chou, A. Amassian, and E. H. Sargent, Nat. Nanotechnol. **7**, 577 (2012).

[6]Z. Chen, S. Berciaud, C. Nuckolls, T. F. Heinz, and L. E. Brus, ACS Nano **4**, 2964 (2010).

[7]L. Gaudreau, K. J. Tielrooij, G. E. D. K. Prawiroatmodjo, J. Osmond, F. J. García de Abajo, and F. H. L. Koppens, Nano Lett. **13**, 2030 (2013).

[8]G. Gómez-Santos and T. Stauber, Phys. Rev. B **84**, 165438 (2011).

[9]R. S. Swathi and K. L. Sebastian, J. Chem. Phys. **130**, 086101 (2009).

[10]K. S. Novoselov, A. K. Geim, S. V. Morozov, D. Jiang, Y. Zhang, S. V. Dubonos, I. V. Grigorieva, and A. A. Firsov, Science **306**(5696), 666 (2004).

[11]A. K. Geim and K. S. Novoselov, Nature Mater. **6**, 183 (2007).

[12]A. C. Neto, F. Guinea, N. M. R. Peres, K. S. Novoselov, and A. K. Geim, Rev. Mod. Phys. **81**(1), 109 (2009).

[13]A. N. Grigorenko, M. Polini, and K. S. Novoselov, Nat. Photonics **6**(11), 749 (2012).

[14]S. Z. Butler, S. M. Hollen, L. Cao, Y. Cui, J. A. Gupta, H. R. Gutiérrez, and J. E. Goldberger, ACS Nano **7**(4), 2898 (2013).

[15]Y. Zhang, Y. W. Tan, H. L. Stormer, and P. Kim, Nature **438**, 201–204 (2005).

[16]C. R. Dean, L. Wang, P. Maher, C. Forsythe, F. Ghahari, Y. Gao, J. Katoch, M. Ishigami, P. Moon, M. Koshino, T. Taniguchi, K. Watanabe, K. L. Shepard, J. Hone, and P. Kim, Nature **497**(7451), 598 (2013).

[17]C. Lee, X. Wei, J. W. Kysar, and J. Hone, Science **321**, 385 (2008).

[18]K. F. Mak, M. Y. Sfeir, Y. Wu, C. H. Lui, J. A. Misewich, and T. F. Heinz, Phys. Rev. Lett. **101**, 196405 (2008).

[19]K. I. Bolotin, K. J. Sikes, Z. Jiang, M. Klima, G. Fudenberg, J. Hone, P. Kim, and H. L. Stormer, Solid State Commun. **146**, 351 (2008).

[20]E. Morales-Narváez, B. Pérez-López, L. B. Pires, and A. Merkoçi, Carbon **50**, 2987 (2012).

[21]S. Jang and Y. C. Cheng, WIREs Comput. Mol. Sci. **3**, 84–104 (2013).

[22]R. Bose, J. Gao, F. W. Sun, J. F. McMillan, A. D. Williams, and C. W. Wong, Opt. Express **17**, 22474 (2009).

[23]M. T. Rakher, R. Bose, C. W. Wong, and K. Srinivasan, Opt. Express **19**, 1786–1793 (2011).

[24]M. Nirmal, B. O. Dabbousi, M. G. Bawendi, J. J. Macklin, J. K. Trautman, T. D. Harris, and L. E. Brus, Nature **383**, 802 (1996).

[25]C. Galland, Y. Ghosh, A. Steinbrück, J. A. Hollingsworth, H. Htoon, and V. I. Klimov, Nat. Commun. **3**, 908 (2012).

[26]C. Galland, Y. Ghosh, A. Steinbrück, J. A. Hollingsworth, V. I. Klimov, and H. Htoon, Nature Commun. **479**, 203–207 (2011).

[27]M. Kuno, D. P. Fromm, H. F. Hamann, A. Gallagher, and D. J. Nesbitt, J. Chem. Phys. **112**, 3117 (2000).

[28]C. H. Crouch, O. Sauter, X. Wu, R. Purcell, C. Querner, M. Drndic, and M. Pelton, Nano Lett. **10**, 1692–1698 (2010).

[29]J. J. Peterson and D. J. Nesbitt, Nano Lett. **9**, 338–345 (2009).

[30]R. R. Nair, P. Blake, A. N. Grigorenko, K. S. Novoselov, T. J. Booth, T. Stauber, N. M. R. Peres, and A. K. Geim, Science **320**, 1308 (2008).

[31]A. Al Salman, A. Tortschanoff, G. Van der Zwan, F. Van Mourik, and M. Chergui, Chem. Phys. **357**, 96 (2009).

[32]N. C. Anderson, M. P. Hendricks, J. J. Choi, and J. S. Owen, J. Am. Chem. Soc. **135**, 18536–18548 (2013).

[33]X. Wang, L. Qu, J. Zhang, X. Peng, and M. Xiao, Nano Lett. **3**(8), 1103 (2003).

[34]Y. Matsumoto, R. Kanemoto, T. Itoh, S. Nakanishi, M. Ishikawa, and V. Biju, J. Phys. Chem. C **112**, 1345 (2008).

[35]R. Bose, J. F. McMillan, J. Gao, C. J. Chen, D. V. Talapin, C. B. Murray, K. M. Rickey, and C. W. Wong, Nano Lett. **8**, 2006–2011 (2008).

[36]M. Liu, H. Zhao, X. Quan, S. Chen, and X. Fan, Chem. Commun. **46**, 7909 (2010).

[37]I. V. Lightcap and P. V. Kamat, J. Am. Chem. Soc. **134**, 7109–7116 (2012).

[38]N. Petrone, C. R. Dean, I. Meric, A. M. van der Zande, P. Y. Huang, L. Wang, D. Muller, K. L. Shepard, and J. Hone, Nano Lett. **12**(6), 2751–2756 (2012).

[39]G. Konstantatos, M. Badioli, L. Gaudreau, J. Osmond, J., Bernechea, F. P. G. Arquer, and F. H. Koppens, Nat. Nanotechnol. **7**(6), 363–368 (2012).